Polymer 50 (2009) 3556–3563

Contents lists available at ScienceDirect

Polymer

journal homepage: www.elsevier.com/locate/polymer

Synthesis of pH-sensitive hollow polymer microspheres and their application as drug carriers

Xiaoying Yang [a,*], Liting Chen [a], Bo Huang [b], Feng Bai [b], Xinlin Yang [b,*]

[a] School of Pharmaceutical Sciences, Tianjin Medical University, Tianjin 300070, China
[b] Key Laboratory of Functional Polymer Materials, Ministry of Education, Institute of Polymer Chemistry, Nankai University, Tianjin 300071, China

ARTICLE INFO

Article history:
Received 16 February 2009
Received in revised form
25 April 2009
Accepted 13 June 2009
Available online 18 June 2009

Keywords:
pH-sensitive hollow polymer microspheres
Distillation precipitation polymerization
Controlled-drug release

ABSTRACT

The pH-sensitive hollow poly(*N*,*N*′-methylene bisacrylamide-*co*-methacrylic acid) (P(MBAAm-*co*-MAA)) microspheres were prepared by a two-stage distillation precipitation polymerization to afford a core–shell poly(methacrylic acid)/poly(*N*,*N*′-methylene bisacrylamide-*co*-methacrylic acid) (PMAA/(P(MBAAm-*co*-MAA))) microsphere with subsequent removal of poly(methacrylic acid) (PMAA) core. PMAA/P(MBAAm-*co*-MAA) core–shell microspheres were synthesized by the second-stage copolymerization of *N*,*N*′-methylene bisacrylamide (MBAAm) as crosslinker and the functional methacrylic acid (MAA) comonomer in acetonitrile with 2,2′-azobisisobutyronitrile (AIBN) as initiator. The pH-responsive properties of hollow P(MBAAm-*co*-MAA) microspheres were investigated by dynamic laser scattering (DLS). The loading and controlled-release behavior of the drug for hollow P(MBAAm-*co*-MAA) microspheres was strongly dependent on the pH values with doxorubicin hydrochloride (DXR) as a model molecule. The core–shell and hollow polymer microspheres were characterized by transmission electron microscopy (TEM), Fourier-transform infrared spectra (FT-IR), DLS and elemental analysis.

1. Introduction

During the last decade, hollow polymer microspheres have attracted much attention due to their wide applications, such as encapsulation for controlled release of drugs and enzymes, fillers, pigments, catalysts, and adsorption materials for sound [1–4]. Significant progress has been made in the design and synthesis of hollow polymer particles by a variety of physical and chemical methods [5–9]. Among them, polymer microspheres with various responsibilities, including pH-sensitive [10–12], thermo-sensitive [13,14], ion-strength [15], magnetism [16], and dual thermo-responsive and ion-recognizable [17], have been prepared by different techniques with wide applications. Environmentally responsive polymer capsules ranging in the size from nanometers to microns have been interesting for the material scientists due to their potential and practical utilization in controlled release [18].

Many functional polymers as drug carriers have been prepared by physical methods from the natural macromolecules, which usually have much broad size distribution [19,20]. The polymer microspheres with uniform size are essential for drug delivery system (DDS) because the distribution of the microspheres in the body and the interaction with biological cells are greatly affected by the particle size [21,22]. Additionally, if monodisperse polymer microspheres are available, the drug release kinetics can be manipulated, therefore making it easier to formulate more sophisticated intelligent DDS. In this context, the synthesis of hollow polymer microspheres with stimuli sensitivity and narrow size distribution warrants further exploration, which will be of both scientific and technical interest.

Doxorubicin chloride (DXR) is a potent antibiotic for treatment of a variety of solid tumors and leukemias [22–25]. However, the cardiotoxicity of this drug is a serious drawback, which limits its direct administration and cumulative storage [23]. The utilization of liposomes as drug delivery vehicles for administering DXR reduces the accumulation of the drug in the heart tissues by decreasing the concentration of free drug in circulation due to the stability of liposomes and their ability to retain the entrapped drug molecules (i.e., minimum leakage) [23,26,27].

In our previous work, monodisperse core–shell polymer microspheres with different functional groups on their surfaces [28,29], hollow polymer microspheres with pyridyl group on the interior surface [30] and thermal sensitivity [14] were prepared by distillation precipitation polymerization in neat acetonitrile. Here, monodisperse pH-responsive poly(*N*,*N*′-methylene bisacrylamide-*co*-methacrylic acid) (P(MBAAm-*co*-MAA)) hollow microspheres with defined size and shell thickness were synthesized by a two-stage distillation precipitation polymerization to afford

* Corresponding authors. Tel.: +86 22 23502023; fax: +86 22 23503510.
E-mail addresses: yangxiaoying@tijmu.edu.cn (X. Yang), xlyang88@nankai.edu.cn (X. Yang).

0032-3861/$ – see front matter © 2009 Elsevier Ltd. All rights reserved.
doi:10.1016/j.polymer.2009.06.027

poly(methacrylic acid)/poly(*N*,*N*′-methylene bisacrylamide-*co*-methacrylic acid) (PMAA/P(MBAAm-*co*-MAA)) core–shell microspheres with subsequent removal of the poly(methacrylic acid) (PMAA) core in water.

2. Experimental

2.1. Materials

N,*N*′-Methylene bisacrylamide (MBAAm, chemical grade, Tianjin Bodi Chemical Engineering Co.) was recrystallized from acetone. Methacrylic acid (MAA) was got from Tianjin Chemical Reagent II Co. and was purified by vacuum distillation. 2,2′-Azobisisobutyronitrile (AIBN, analytical grade) was available from Chemical Factory of Nankai University and was recrystallized from methanol. Acetonitrile (analytical grade, Tianjin Chemical Reagents II Co.) was dried over 4 Å molecule sieves and purified by distillation. Doxorubicin hydrochloride (DXR) was provided by Beijing Huafeng United Technology Co. and used as received. Dialysis chamber for the drug release was purchased from Beijing Dingguo Biotech Co. ($\Phi = 36$ mm), which had a molecule weight cut-off of 8000–15 000 g/mol. The other reagents were analytical grade and used without any further purification.

2.2. Preparation of core–shell microspheres

Monodisperse polymethacrylic acid (PMAA) microspheres were prepared according to the procedure in our previous work by distillation precipitation polymerization in acetonitrile with AIBN as initiator in the absence of any crosslinker or stabilizer [31], which was considered as the first-stage polymerization in the present work.

Monodisperse poly(methacrylic acid)/poly(*N*,*N*′-methylene bisacrylamide-*co*-methacrylic acid) (PMAA/P(MBAAm-*co*-MAA)) core–shell microspheres were synthesized in the presence of PMAA microspheres as seeds by the second-stage distillation precipitation polymerization of MAA and MBAAm crosslinker with AIBN as initiator in acetonitrile. In a typical experiment, PMAA seeds (0.35 g), 0.10 g of MBAAm crosslinker, 0.15 g of MAA comonomer and 0.005 g of AIBN (2 wt% of the total comonomers) were added in 40 mL of acetonitrile at room temperature in a 50 mL of two-necked flask equipped with a fractionating column, Liebig condenser and a receiver. The flask was submerged in a heating mantle and the second-stage polymerization mixture was heated from ambient temperature to the boiling state within 15 min. Then the solvent was distilled out of the reaction system and the polymerization was ended after 20 mL of acetonitrile was distilled off the reaction system within 70 min. After the polymerization, the resultant PMAA/P(MBAAm-*co*-MAA) core–shell microspheres were purified by ultracentrifugation and washed with acetonitrile for three times.

The PMAA/P(MBAAm-*co*-MAA) core–shell microspheres with different shell thicknesses and crosslinking degrees of P(MBAAm-*co*-MAA) shell layer were conveniently prepared by the second-stage distillation precipitation copolymerization via altering the amount of MAA comonomer and MBAAm crosslinker, while the amount of AIBN initiator was maintained at 2 wt% relative to the total comonomers. The crosslinking degree was referred as weight percent of MBAAm crosslinker relative to the total comonomers of MBAAm and MAA used for the second-stage polymerization in the present work. The treatment of these core–shell microspheres was the same as that for the typical procedure.

2.3. Preparation of monodisperse hollow P(MBAAm-co-MAA) microspheres

The PMAA/P(MBAAm-*co*-MAA) core–shell microspheres were dispersed in ethanol and the non-crosslinked PMAA cores were selectively removed to afford the corresponding P(MBAAm-*co*-MAA) hollow microspheres after stirring. The hollow P(MBAAm-*co*-MAA) microspheres were subsequently redispersed in ethanol, followed by washing with ethanol and centrifugation for three times to remove the residual PMAA segments.

2.4. The drug loading and release behavior of the hollow P(MBAAm-co-MAA) microspheres as the drug vehicle

A series of DXR solutions with different initial concentrations were mixed with respect of the same concentration of hollow microspheres (0.4 mg/mL). The loading of the drug took place in the suspension on an SHA-B shaker with gentle agitation by rolling the bottles in a horizontal position to approximately 40 rpm for 24 h. The unloaded DXR molecules were removed by ultracentrifugation. The loading capacity of DXR on P(MBAAm-*co*-MAA) hollow microspheres was determined by ultraviolet spectra (UV) at wavelength of 233 nm, which was calculated by the difference of DXR concentration between the original DXR solution and the supernatant after loading. In this process, the supernatant after ultracentrifugation in the presence of P(MBAAm-*co*-MAA) hollow microspheres without DXR was utilized as a blank sample for determination, in which the DXR concentration was calibrated from a standard curve of DXR aqueous solution. The loading of DXR on P(MBAAm-*co*-MAA) hollow microspheres at pH values of 1 and 10 were determined by the same method.

The P(MBAAm-*co*-MAA) hollow microspheres (6.9 mg) loaded with DXR under the neutral conditions were dispersed in 3 mL aqueous solution and the dispersion was divided into three equal aliquots. The drug-loaded hollow P(MBAAm-*co*-MAA) samples used for the release experiments were placed into the dialysis chambers, which were dialyzed in 80 mL of aqueous solution under different pH environments, such as pH = 1, 7, 10, respectively. The drug release was assumed to start as soon as the dialysis chambers were placed into the reservoir. The release reservoir was kept under constant stirring, and at various time points, one of the dialysis chambers was taken out for characterization. The concentration of DXR released from P(MBAAm-*co*-MAA) hollow microspheres into aqueous solution was quantitatively analyzed by UV spectroscopy at wavelength of 233 nm. The dialysate from basic solutions were analyzed after adjusting to pH 6–7 with 1.0 M HCl.

The pH of the solution for loading and release process was adjusted by either 1.0 M NaOH or 1.0 M HCl aqueous solution.

2.5. Characterization

The morphology of the resultant polymer microspheres was determined by transmission electron microscopy (TEM) using a Technai G^2 20-S-TWIN microscope. Samples for TEM characterization were dispersed in solvent and a drop of the dispersion was spread onto the surface of a copper grid coated with a carbon membrane and then dried in vacuum at room temperature for characterization.

All the size and size distribution reflect the averages of about 100 particles, which are calculated according to the following formula:

$$U = D_W/D_n; D_n = \sum_{i=1}^{k} n_i D_i / \sum_{i=1}^{k} n_i;\ D_w = \sum_{i=1}^{k} n_i D_i^4 / \sum_{i=1}^{k} n_i D_i^3$$

where U is the polydispersity index, D_n is the number-average diameter, D_w is the weight-average diameter, D_i is the particle diameter of the determined microparticles.

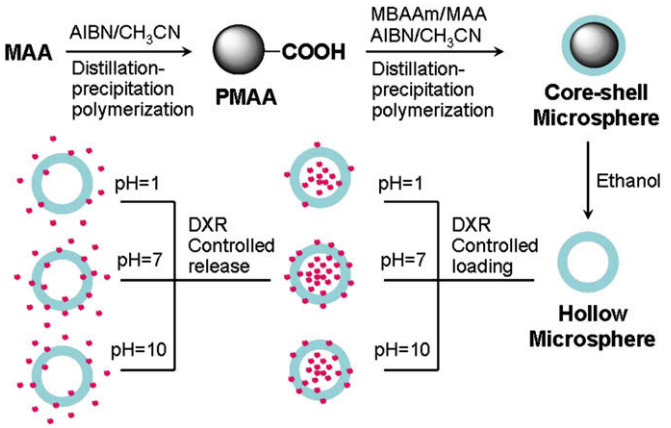

Scheme 1. Preparation of pH-sensitive P(MBAAm-*co*-MAA) hollow microspheres and their controlled loading and release behavior as drug reservoir.

Fourier-transform infrared spectra were determined on a Bruker Tensor 27 FT-IR spectrometer over potassium bromide pellet and the diffuse reflectance spectra were scanned over the range of 4000–400 cm^{-1}.

UV–vis absorption spectra were measured on a JASCO V-570 UV–vis spectrometer with a laser source of wavelength at 233 nm as an excitation source for the determination of the concentration of DXR.

Elemental analysis (EA) was performed on a Perkin–Elmer-2400 to determine the nitrogen, carbon and hydrogen contents of the resultant polymer particles.

Dynamic light scattering (DLS) and static light scattering (SLS) measurements were performed in a laser scattering spectrometer (BI-200 SM) equipped with a digital correlation (BI-10000 AT) at 636 nm. All the samples were prepared from the suspension with concentration of about 10 μg/mL after ultrasonic irradiation and were then measured at pH = 2, 7, 12, respectively. The hydrodynamic diameter (D_h) and the polydispersity index of the size distribution were obtained by a cumulant analysis.

3. Results and discussion

Scheme 1 illustrated the preparation of PMAA/P(MBAAm-*co*-MAA) core–shell microspheres by two-stage distillation precipitation polymerization, further development of hollow P(MBAAm-*co*-MAA) microspheres and the pH-dependent drug-release behavior of the resultant hollow P(MBAAm-*co*-MAA) microspheres.

The TEM micrograph of PMAA microspheres by the first-stage distillation precipitation polymerization is shown in Fig. 1A, which indicated that the polymer microspheres had spherical shape and smooth surface with an average size of 95 nm and a polydispersity index (U) of 1.008 as listed in Table 1.

3.1. Preparation of PMAA/P(MBAAm-co-MAA) core–shell microspheres

In the present work, the PMAA microspheres without any crosslinker were used as the templates for the synthesis of PMAA/P(MBAAm-*co*-MAA) core–shell microspheres. The results have demonstrated that acetonitrile was a suitable medium for the efficient hydrogen-bonding interaction between carboxylic acid group and pyridyl group [30] as well as the synergic hydrogen-bonding interaction between the carboxylic acid group and amide group [32] acting as a driving force for the building raspberry-like polymer composites. Here, the synergic hydrogen-bonding interaction between the carboxylic acid groups on the surface of PMAA seeds and the carboxylic acid group of MAA monomer as well as the amide group of MBAAm crosslinker played a key role for the formation of monodisperse PMAA/P(MBAAm-*co*-MAA) core–shell microspheres as shown in Scheme 1. The preparation of monodisperse PMAA microspheres by distillation precipitation polymerization in acetonitrile was reported in our previous paper, in which the growth

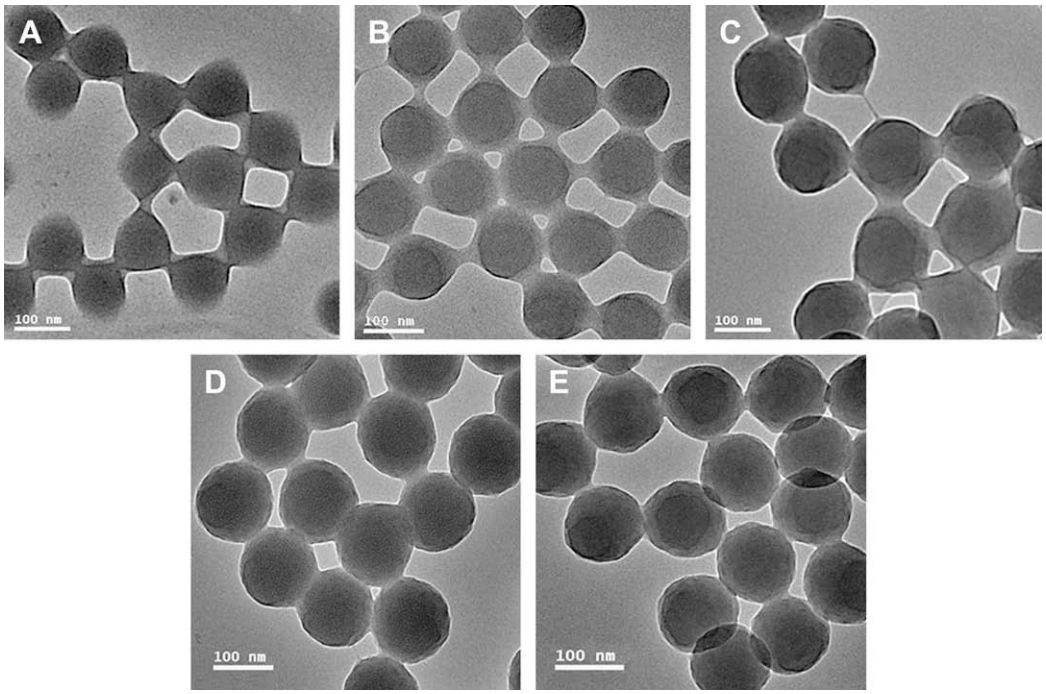

Fig. 1. TEM micrographs of polymer microspheres: (A) PMAA seed; (B) PMAA/P(MBAAm-*co*-MAA) core–shell microspheres with crosslinking degree of 32 wt%; (C) PMAA/P(MBAAm-*co*-MAA) core–shell microspheres with crosslinking degree of 40 wt%; (D) PMAA/P(MBAAm-*co*-MAA) core–shell microspheres with crosslinking degree of 50 wt%; (E) PMAA/P(MBAAm-*co*-MAA) core–shell microspheres with crosslinking degree of 60 wt%.

Table 1
Reaction conditions, size and size distribution of PMAA core microspheres, and PMAA/P(MBAAm-*co*-MAA) core–shell microspheres.[a]

Entry	Crosslinking degree (wt%)	D_n (nm)	D_w (nm)	U	Shell thickness[a] (nm)
PMAA	–	95	96	1.008	–
CS-1	32	111	112	1.003	8
CS-2	40	147	148	1.005	26
CS-3	50	164	165	1.006	35
CS-4	60	156	157	1.006	30
H-1	32	155	158	1.021	8
H-2	40	184	187	1.017	26

[a] Shell thickness as the half of the difference between the diameter of PMAA/P(MBAAm-*co*-MAA) core–shell microspheres and that of the corresponding PMAA core.

mechanism of PMAA microspheres with the aid of efficient hydrogen-bonding interaction was investigated in detail [31].

The formation of P(MBAAm-*co*-MAA) shell with different crosslinking degree was designed to investigate the effect of MBAAm crosslinker for the second-stage copolymerization, in which the crosslinking degrees were varied from 32 to 60 wt% with MAA feed keeping at 3/7 (relative to the mass of PMAA seeds). The TEM micrographs of the resultant PMAA/P(MBAAm-*co*-MAA) core–shell microspheres with different crosslinking degrees are shown in Fig. 1B–E. These results indicated that the polymer microspheres had spherical shape with smooth surface, which confirmed the core–shell structure of the final polymer microspheres with different contrast for the core and shell segments, especially in the case of higher crosslinking degree (>40 wt%) as identified in Fig. 1C–E. Further, the results revealed that the polymer microspheres had spherical shape with core–shell structure and occurrence as multiplet particles in TEM observation (Fig. 1A–C), which may be due to the strong interparticle hydrogen-bonding interaction and soft surface of the PMAA/P(MBAAm-*co*-MAA) core–shell microspheres in the case of low crosslinking degree of MBAAm (lower than 40 wt%).

The reaction conditions, size and size distribution of the resultant PMAA/P(MBAAm-*co*-MAA) core–shell microspheres with various MBAAm crosslinking degrees for the synthesis of shell layer are summarized in Table 1. The average diameters were considerably increased from 95 nm of PMAA core to 111, 147 and 164 nm of the resultant PMAA/P(MBAAm-*co*-MAA) core–shell microspheres, while the crosslinking degree was enhanced from 32 to 50 wt%. When MBAAm crosslinking degree was increased further to 60 wt%, the diameter of PMAA/P(MBAAm-*co*-MAA) core–shell microsphere was slightly decreased to 156 nm which may be due to the shrinking effect of the polymer particles in the case of high crosslinking degree (60 wt%). All the PMAA/P(MBAAm-*co*-MAA) core–shell microspheres had narrow size distribution without formation of second-stage copolymerization, which indicated that the P(MBAAm-*co*-MAA) shell layer was successfully encapsulated onto PMAA seeds with the efficient hydrogen-bonding interaction between the carboxylic acid group of PMAA seeds and the carboxylic acid group of MAA monomer as well as the amide group of MBAAm crosslinker. These were similar to the results reported in our previous papers [14,30,31]. The larger diameters of the resultant PMAA/P(MBAAm-*co*-MAA) core–shell microspheres were originated from the higher yields with increasing MBAAm crosslinking degree (from 32 to 50 wt%) for the second-stage copolymerization as summarized in Table 1, as the number of the polymer microspheres was maintained constant in the absence of any second-initiated particles after the second-stage polymerization. Such results were consistent with the effects of monomer loadings and crosslinking degree on the size and the yield of poly(divinylbenzene) (PDVB) microspheres by distillation precipitation polymerization in our previous work [33].

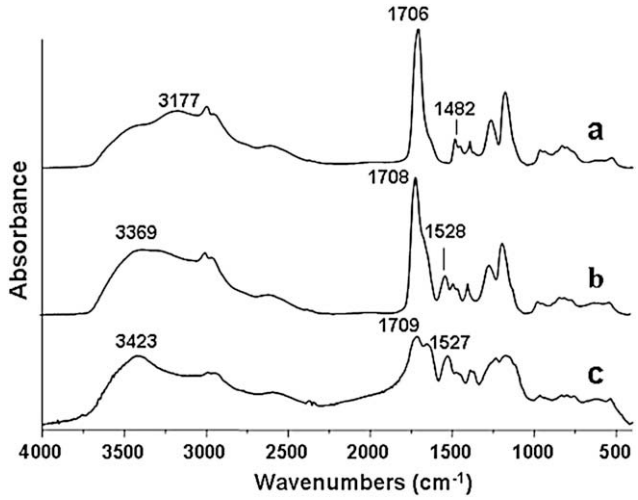

Fig. 2. FT-IR spectra of polymer microspheres: (a) PMAA seeds; (b) PMAA/P(MBAAm-*co*-MAA) core–shell microspheres; (c) hollow P(MBAAm-*co*-MAA) microspheres.

The seeded copolymerizations of MBAAm and MAA leading to PMAA/P(MBAAm-*co*-MAA) core–shell microspheres was studied by FT-IR spectra as shown in Fig. 2. In addition to the peak at 1708 cm^{-1} assigning to the characteristic stretching vibration of the carbonyl unit in PMAA segments, the FT-IR spectrum of PMAA/P(MBAAm-*co*-MAA) core–shell microspheres in Fig. 2b had a new peak at 1528 cm^{-1} assigning to the vibration of the amide group of PMBAAm segments. The elemental analysis in Table 2 indicated that the N content of PMAA core was only 0.63% (the residual part of AIBN initiator) and that of PMAA/P(MBAAm-*co*-MAA) microspheres was significantly enhanced to 3.01% (with crosslinking degree of 40 wt%), which confirmed the core–shell structure of the final polymer microspheres after the second-stage polymerization with the presence of PMBAAm components on the shell layer.

3.2. Monodisperse P(MBAAm-co-MAA) hollow microspheres

PMAA cores of the resultant PMAA/P(MBAAm-*co*-MAA) core–shell microspheres were selectively removed by the dissolution in ethanol to afford P(MBAAm-*co*-MAA) hollow microspheres. The typical TEM micrographs of P(MBAAm-*co*-MAA) hollow microspheres with different crosslinking degrees are shown in Fig. 3A and B, in which convincing hollow-sphere structures were observed with the presence of circular rings of sectional spheres and a cavity in the interior. These results demonstrated that P(MBAAm-*co*-MAA) shell layers with thicknesses of 8 and 26 nm (Entries H1 and H2 in Table 1) were strong enough to support the resultant voids during the selective removal of PMAA cores by dissolution. The diameters of hollow P(MBAAm-*co*-MAA) microspheres with crosslinking degrees of 32 and 40 wt% as summarized in Entries H1 and H2 in Table 1 were a little larger than the corresponding core–shell polymer microspheres, which was due to the swollen effect of the hollow polymer microspheres during the selective removal of non-crosslinking PMAA core. Both P(MBAAm-

Table 2
The elemental analysis of the polymer microspheres.

Entry	N (%)
PMAA	0.63
PMAA/P(MBAAm-*co*-MAA) core–shell microspheres[a]	3.01
P(MBAAm-*co*-MAA) hollow microspheres[b]	7.59

[a] PMAA/P(MBAAm-*co*-MAA) core–shell microspheres with 40 wt% crosslinking degree.
[b] P(MBAAm-*co*-MAA) hollow microspheres with 40 wt% crosslinking degree.

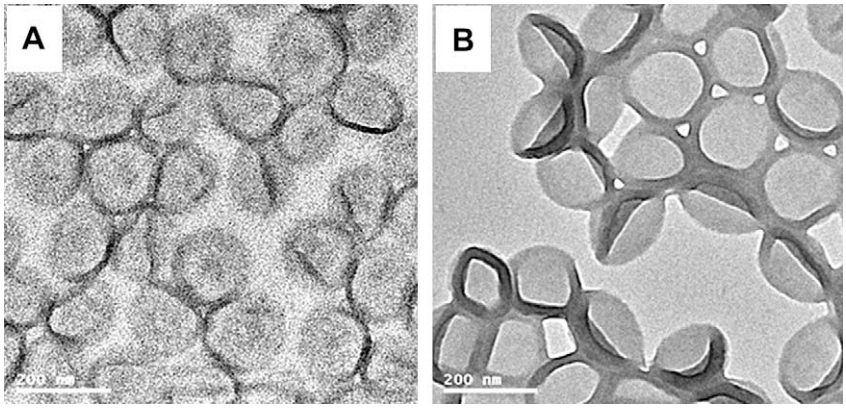

Fig. 3. TEM micrographs of hollow P(MBAAm-*co*-MAA) microspheres: (A) crosslinking degree of 32 wt% with shell thickness of 8 nm; (B) crosslinking degree of 40 wt% with shell thickness of 26 nm.

co-MAA) hollow microspheres occurred as multiplet with some coagula as shown by TEM images in Fig. 3, which was due to the strong interparticle hydrogen-bonding interaction and soft surface of the hollow polymer microspheres. This would be discussed further in the present paper.

The considerable decrease of the peak at 1708 cm^{-1} corresponding to the carbonyl unit of carboxylic acid group of PMAA segments in FT-IR spectrum of P(MBAAm-*co*-MAA) hollow microspheres as shown in Fig. 2c, the presence of the strong-wide peaks at 3423 cm^{-1} assigning to the characteristic peak of vibration of N–H unit and the higher peak at 1527 cm^{-1} due to the stretching vibration of carbonyl group of amide group in PMBAAm segment proved the successful removal of the PMAA core by dissolution in ethanol. The nitrogen content of hollow P(MBAAm-*co*-MAA) microspheres (with crosslinking degree of 40 wt%) was considerably increased from 3.01% of PMAA/P(MBAAm-*co*-MAA) core–shell microspheres to 7.59% as listed in Table 2, which implied that the shell of hollow polymer microspheres was composed of P(MBAAm-*co*-MAA) network. The driving force for such selective removal of PMAA in ethanol at room temperature to afford hollow P(MBAAm-*co*-MAA) microspheres was based on the good solubility of the non-crosslinked PMAA cores, which was much mild and environmentally friendly without utilization of highly corrosive reagent, such as hydrofluoric acid (HF) in the case of silica as sacrificial core [28,29].

All these results proved the preparation of PMAA/P(MBAAm-*co*-MAA) core–shell microspheres by two-stage distillation precipitation polymerization and the subsequent development of hollow P(MBAAm-*co*-MAA) after the selective dissolution of the non-crosslinked PMAA core. The present approach via using hydrogen-bonding interaction to form core–shell structure without any additive has the advantage that it is much easier and simpler than some complex modification processes of template, such as attaching an initiator onto the silica surface to achieve a controlled living polymerization [34], modification of silica template with 3-(trimethoxysilyl)propyl methacrylate (MPS) [27,28], and polystyrene particles with concentrated sulfuric acid [35].

The pH–stimuli volume transition of P(MBAAm-*co*-MAA) hollow microspheres by DLS measurements is summarized in Table 3. The extreme large hydrodynamic diameter (>2600 nm) of hollow P(MBAAm-*co*-MAA) microspheres at pH of 2 was originated from the strong interparticle hydrogen-bonding interaction between the carboxylic acid groups as well as amide groups of P(MBAAm-*co*-MAA) under acid conditions. Further, the hydrodynamic diameters at pH of 2 were in an undulation state indicating the resultant coagulum of P(MBAAm-*co*-MAA) hollow particles via hydrogen-bonding interaction in a dynamic equilibrate state, which may be due to the nature of the hydrogen-bonding as a weak secondary-level interaction. These results can give a good explanation for occurrence of hollow P(MBAAm-*co*-MAA) microspheres as multiplet with some coagula as observed by TEM characterization in the present work. The hydrodynamic diameters of hollow P(MBAAm-*co*-MAA) microspheres at pH of 7 were 161 and 192 nm with crosslinking degree of 32 and 40 wt%, which were a little larger than those of 155 and 184 nm from TEM observation. Such results also confirmed the hydrophilic property of the resultant P(MBAAm-*co*-MAA) hollow microspheres, as the former ones were obtained from swollen states. When the pH was adjusted to 12, the hydrodynamic sizes of P(MBAAm-*co*-MAA) hollow microspheres were increased considerably to 211 and 228 nm with MBAAm crosslinking degrees of 32 and 40 wt%, respectively. These changes in size were due to the partial ionization of the carboxylic acid groups in PMAA segment of the P(MBAAm-*co*-MAA) shell under high pH values, resulting in Donnan osmotic swelling of P(MBAAm-*co*-MAA) network. The structure of the hollow polymer shell can be switched reversibly from a collapsed to a highly swollen state under different pH conditions.

A combination of DLS and SLS measurements affording the ratio of average gyration radium to the corresponding average hydrodynamic radius (R_g/R_h) is listed in Table 4. It is well known that the R_g/R_h values reflect the morphology or conformation of the polymer chains or the density distribution of the polymer particles in the solution [36,37]. The R_g/R_h values of P(MBAAm-*co*-MAA) hollow microspheres with crosslinking degree of 32 and 40 wt% were kept at 1.09 and 1.28 under pH of 12, which was considerably higher

Table 3
The hydrodynamic diameters of hollow P(MBAAm-*co*-MAA) microspheres under different pH conditions.[a]

Entry	pH = 2 (nm)	pH = 7 (nm)	pH = 12 (nm)
H-1	3938	161	211
H-2	2639	192	228

[a] Hydrodynamic diameters from DLS determined at scattering angle of 90° at pH value of 12.

Table 4
The drug loading capacity and encapsulation efficiency with different initial DXR concentrations.

Entry	D_h[a] (nm)	R_g[b] (nm)	R_g/R_h	U
H-1	216.3	117.8	1.09	1.005
H-2	247.9	159.2	1.28	1.167

[a] Value from DLS determined at scattering angle of 90° at pH value of 12.
[b] SLS measurement performed from 50 to 125° at pH value of 12.

than the typical value of 0.774 for the uniform microspheres. These results implied that the resultant P(MBAAm-*co*-MAA) particles had a hollow structure, which were in accordance with the results from TEM observation, FT-IR characterization and elemental analysis.

3.3. Loading and releasing behavior of DXR on P(MBAAm-co-MAA) hollow microspheres

To evaluate the potential application of P(MBAAm-*co*-MAA) hollow microspheres as a drug carrier, DXR was used as the model molecule to perform the loading and releasing test, in which the hollow polymer microspheres with the crosslinking degree of 40 wt% with shell thickness of 26 nm was used as a sample. The drug loading capacity and the encapsulation efficiency of the hollow P(MBAAm-*co*-MAA) microspheres were calculated according to the following formula:

$$\text{Drug loading capacity} = (W_{\text{administered dose}} - W_{\text{residual dose insolution}})/W_{\text{hollow microspheres}}$$

$$\text{Encapsulation efficiency} = (W_{\text{administered dose}} - W_{\text{residual dose in solution}})/W_{\text{administered dose}} \times 100\%$$

The loading capacity and encapsulation efficiency of DXR incorporated onto the hollow P(MBAAm-*co*-MAA) microspheres were obtained at different initial DXR concentrations with respect of the same concentration of hollow polymer microspheres (0.4 mg/mL) via the analysis of the residual DXR concentration remaining in the solution during the loading process. The results in Table 5 revealed that the loading capacity of the DXR on hollow P(MBAAm-*co*-MAA) microspheres was increased quickly from 172 μg/mg to 357 μg/mg with increasing the initial DXR concentration from 83 to 304 μg/mL, while the encapsulation efficiencies of DXR were considerably decreased from 83 to 47%. In the present work, the initial concentration of DXR at 138 μg/mL was considered as an appropriate value for loading process as the loading capacity (282 μg/mg) and encapsulation efficiency (82%) were comparatively high in this case.

The pH sensitivity of polymer microspheres or micelles with DXR as a model drug has been studied in the literature [11,12]. However, the detailed mechanism for this property was not well explained in these papers. Herein, the loading behavior DXR on hollow P(MBAAm-*co*-MAA) microspheres was investigated in detail under different pH environments as shown in Fig. 4 with the initial DXR concentration of 182 μg/mL. The loading capacity of DXR on hollow P(MBAAm-*co*-MAA) microspheres were 40 μg/mg at pH of 1, 321 μg/mg at pH of 7 and 236 μg/mg at pH of 10, respectively. In other words, pH values of the environment had significant effect on the loading capacity of the DXR for hollow P(MBAAm-*co*-MAA) microspheres.

The surface structure of hollow P(MBAAm-*co*-MAA) microspheres had carboxylic acid groups and amide groups with strong polarity and the molecule structure of DXR had three hydroxyl groups and an amino group with strong polarity as shown in Scheme 2. All these groups may participate in the formation of hydrogen-bonding interaction during the loading process of DXR on hollow P(MBAAm-*co*-MAA) microspheres under suitable conditions.

Table 5
DLS and SLS results of hollow P(MBAAm-*co*-MAA) microspheres.

Initial DXR concentration (μg/mL)	82.9	138.1	185.8	248.6	303.8
Loading capacity of DXR (μg/mg)	172.0	281.6	302.1	326.2	357.3
Encapsulation efficiency (%)	83.0	81.6	56.9	52.5	47.0

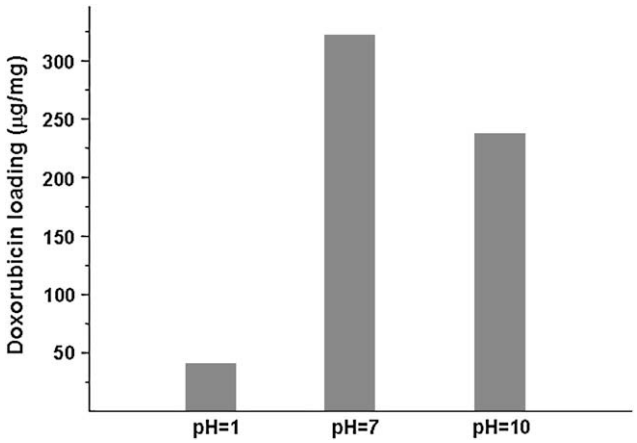

Fig. 4. The loading capacity of DXR on hollow P(MBAAm-*co*-MAA) microspheres with shell thickness of 26 nm under different pH conditions.

The results in Fig. 4 indicated that the highest loading capacity (321 μg/mg) of DXR on hollow P(MBAAm-*co*-MAA) microspheres was afforded under neutral conditions, rather than under either acid or basic conditions. Under neutral conditions, four kinds of hydrogen-bonding interaction between the host P(MBAAm-*co*-MAA) hollow microspheres and guest DXR molecules may be formed, i.e., carboxylic acid group of PMAA segment with the hydroxyl group of DXR, carboxylic acid group of PMAA segment with amino group of DXR, amide group of PMBAAm segment and hydroxyl group of DXR, as well as the amide group of PMBAAm segment with amino group of DXR. Under acid conditions, the amino group of DXR was protonated as $-NH_3^+$ form, which cannot play an active role for the hydrogen-bonding interaction. In such case, two kinds of hydrogen-bonding interaction may occur between the host P(MBAAm-*co*-MAA) hollow microspheres and guest DXR molecules, i.e., carboxylic acid group of PMAA segment with the hydroxyl group of DXR, and amide group of PMBAAm segment and hydroxyl group of DXR. Further, the amide group of PMBAAm segment may be partially protonated under strong acid conditions, which would weaken the hydrogen-bonding interaction between amide group and hydroxyl group of DXR drug. While under basic conditions, the carboxylic acid groups of PMAA segment can be ionized as carboxylate anion species, which cannot take part in the hydrogen-bonding interaction with the hydroxyl or amino groups of DXR. In such a way, two kinds of hydrogen-bonding interaction can be formed between the host P(MBAAm-*co*-MAA) hollow microspheres and guest DXR molecules, i.e., amide group of PMBAAm segment and hydroxyl group of DXR, as well as the amide group of PMBAAm segment with amino group of DXR. The functional groups of host P(MBAAm-*co*-MAA) hollow

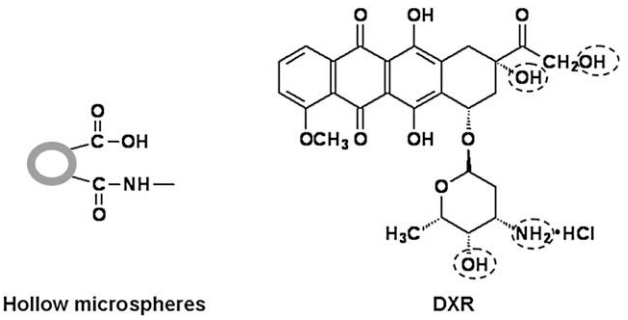

Scheme 2. Surface structure of P(MBAAm-*co*-MAA) hollow microspheres and chemical structure of DXR molecule.

Table 6
Functional groups for the formation of efficient hydrogen-bonding interaction between host P(MBAAm-*co*-MAA) hollow microspheres and guest DXR molecule under different pH conditions.

	Hollow microspheres	DXR
pH = 1	–COOH	–OH
pH = 7	–COOH, –CONH	–OH, $–NH_2$
pH = 10	–CONH	–OH, $–NH_2$

microspheres and guest DXR drug molecule can efficiently participate in the hydrogen-bonding interaction under different pH conditions are summarized in Table 6. Therefore, the strongest hydrogen-bonding interaction between hollow P(MBAAm-*co*-MAA) microspheres and DXR drug was formed under neutral condition and the most efficient loading process of DXR on hollow P(MBAAm-*co*-MAA) microspheres was afforded in such case. The larger loading capacity of DXR under basic condition than that under acid condition for hollow P(MBAAm-*co*-MAA) microspheres implied that the hydrogen-bonding interaction was stronger in the former case.

The controlled-drug releasing behavior of DXR loaded onto hollow P(MBAAm-*co*-MAA) microspheres was investigated under different pH environments with the same initial loading capacity of 272 μg/mg as shown in Fig. 5. The DXR released very slowly from hollow P(MBAAm-*co*-MAA) microspheres and the releasing rate leveled off after 4 h under neutral condition (pH = 7). In such case, only about 15% of the loaded DXR was released from hollow P(MBAAm-*co*-MAA) microspheres even after 24 h. 35% and 98% of the total loaded DXR drugs on hollow P(MBAAm-*co*-MAA) microspheres were released at pH of 10 and 1, respectively, which were much faster than the releasing rate under neutral conditions as illustrated in Fig. 5. The considerable dependence of the releasing behavior of DXR drug from hollow P(MBAAm-*co*-MAA) microspheres on pH values in the environment may be originated from the difference of the strength for the hydrogen-bonding interaction between the host P(MBAAm-*co*-MAA) hollow microspheres and guest DXR drug molecule under different pH conditions, which has been discussed in detail for the drug loading process of DXR on hollow P(MBAAm-*co*-MAA) microspheres.

The effect of pH on the loading and releasing behavior of the DXR for the hollow P(MBAAm-*co*-MAA) microspheres via hydrogen-bonding interaction mechanism was investigated further by the FT-IR spectra as shown in Fig. 6. From the FT-IR spectra, the bands at

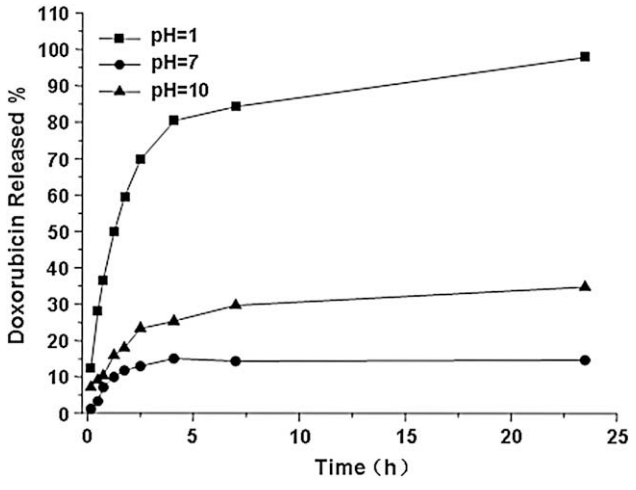

Fig. 5. The controlled release of DXR from hollow P(MBAAm-*co*-MAA) microspheres with shell thickness of 26 nm under different pH conditions.

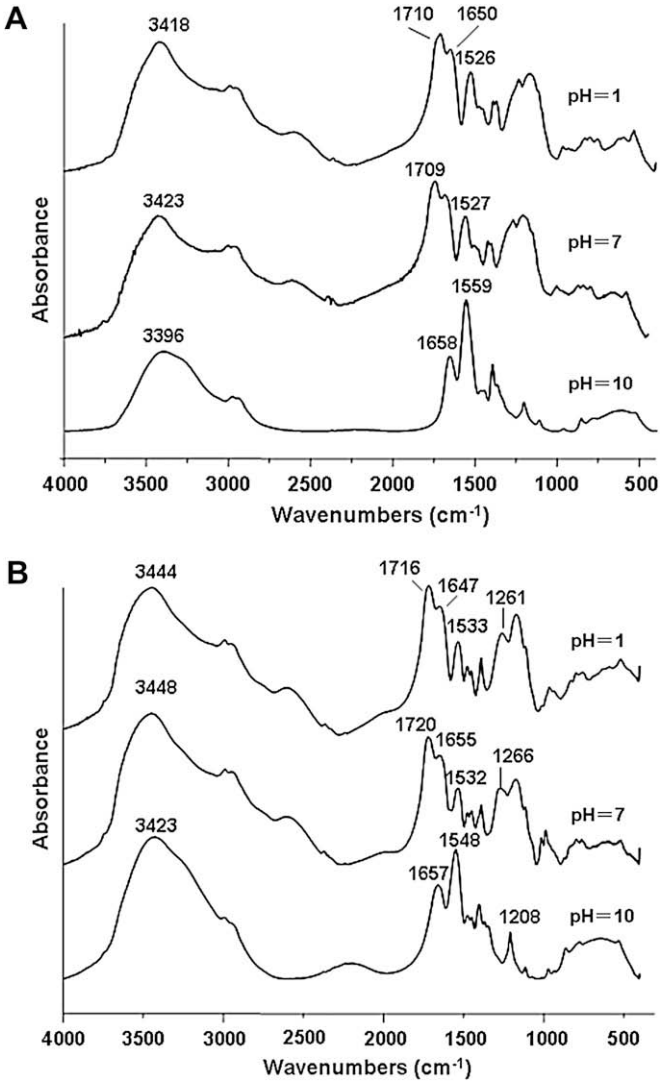

Fig. 6. FT-IR spectra of hollow P(MBAAm-*co*-MAA) microspheres under different pH environments: (A) before loading DXR; (B) after loading DXR.

1559 and 1548 cm^{-1} assigning to the typical absorption of the carboxylate were clearly observed for the hollow spheres before and after loading of DXR molecule, which indicated the ionization of the carboxylic acid groups under basic conditions. In the acid environment, the absorption peak at 1710 cm^{-1} of the carboxylic acid groups before loading the DXR drug was changed to 1716 cm^{-1} after loading of the drug molecule. While under near neutral condition, the absorption peak at 1709 cm^{-1} of the carboxylic acid groups before loading the DXR drug was changed to 1720 cm^{-1} after loading of the drug molecule. These changes in FT-IR spectra may be caused by the hydrogen-bonding interaction between the hollow spheres and the DXR molecule. These results were consistent with the results reported in the literature [38,39].

4. Conclusion

The monodisperse pH-sensitive hollow P(MBAAm-*co*-MAA) microspheres with size below 200 nm and shell thickness in the range of 8–26 nm were prepared by the selective dissolution of non-crosslinked PMAA core in ethanol from the corresponding PMAA/P(MBAAm-*co*-MAA) core–shell microspheres, which were synthesized by a two-stage distillation precipitation polymerization. The

P(MBAAm-*co*-MAA) microspheres with hollow structures were confirmed by the results from TEM observation, FT-IR spectra, DLS and SLS characterization. The investigation of the *in-vitro* loading and release behavior demonstrated that the hollow P(MBAAm-*co*-MAA) microspheres toward DXR drug possessed good loading capacity (as high as 357 μg/mg) with high encapsulation efficiency (as high as 83%). The loading and release behavior of DXR drug with hollow P(MBAAm-*co*-MAA) microsphere as a reservoir was highly dependent on the pH values in the environment, which can be well interpreted by the difference in strength of the hydrogen-bonding interaction between the host P(MBAAm-*co*-MAA) hollow microspheres and the guest DXR drug under different pH conditions. The results imply that P(MBAAm-*co*-MAA) hollow microspheres may have a potential application as a reservoir for the controlled release.

Acknowledgement

This work was supported by the National Natural Science Foundation of China with contract no.: 20874049 and National Science Foundation of Tianjin City with contract no.: 07JCYBJC01700.

References

[1] Zhang J, Xu S, Kumacheva E. J Am Chem Soc 2004;126:7908.
[2] Cochran JK. Curr Opin Solid State Mater Sci 1998;3:474.
[3] Gill I, Ballesteros A. J Am Chem Soc 1998;120:8587.
[4] Caruso F. Adv Mater 2001;13:11.
[5] McDonald CJ, Bouck KJ, Chaupt AB, Stevens CJ. Macromolecules 2000;33:1593.
[6] Xu XL, Asher SA. J Am Chem Soc 2004;126:7940.
[7] Pavlyuchenko VN, Sorochinskaya OV, Ivanchev SS, Klubin VV, Kreichman GS, Budtov VP, et al. J Polym Sci Part A Polym Chem 2001;39:1435.
[8] Zha LS, Zhang Y, Yang WL, Fu SK. Adv Mater 2002;14:1090.
[9] Mandal TK, Fleming MS, Walt DR. Chem Mater 2000;12:3481.
[10] Li GL, Liu G, Kang ET, Neoh KG, Yang XL. Langmuir 2008;24:9050.
[11] Lee ES, Na K, Bae YH. J Controlled Release 2005;103:405.
[12] Leroux JC, Roux E, Garrec DL, Hong K, Drummond DC. J Controlled Release 2001;72:71.
[13] Weda P, Trzebicka B, Dworak A, Tsvetanov CB. Polymer 2008;49:1467.
[14] Li GL, Yang XY, Wang B, Wang JY, Yang XL. Polymer 2008;49:3436.
[15] Ibarz G, Dahen L, Donath E, Möhwald H. Adv Mater 2001;13:1324.
[16] Huang JS, Wan SR, Guo M, Yan HS. J Mater Chem 2006;16:4535.
[17] Ju XJ, Liu L, Xie R, Niu CH, Chu LY. Polymer 2009;50:922.
[18] Gao HF, Yang WL, Wang CH, Fu SK. Polymer 2005;46:1087.
[19] Yun YH, Goetz DJ, Yellen P, Chen WL. Biomaterials 2004;25:147.
[20] Zhou QZ, Wang LY, Ma GH, Su ZG. J Colloid Interface Sci 2007;311:118.
[21] Chattopadhygay P, Shakunov BY, Yim D, Cipolla D, Boyd B, Farr S. Adv Drug Deliv Rev 2007;59:444–53.
[22] Shiga G, Muramatsu N, Kondo T. J Pharm Pharmacol 1996;48:891.
[23] Brown MD, Schatzlein A, Brownlie A, Jack V, Wang W, Tettley L, et al. Bioconjug Chem 2000;11:880.
[24] Son YJ, Jang JS, Cho YW, Chung H, Park RV, Kwon IC, et al. J Control Release 2003;91:135.
[25] Kabanov AV, Batrakova EV, Alakhov VY. J Controlled Release 2003;91:75.
[26] Satsuka Y, Nakade A, Tsuruda T, Sonobe T. J Controlled Release 2003;91:271.
[27] Mayer LD, Cullis DR, Bally MB. J Liposome Res 1994;4:529.
[28] Liu GY, Zhang H, Yang XL, Wang YM. Polymer 2007;47:5896.
[29] Liu GY, Li LY, Yang XL, Dai Z. Polym Adv Technol 2008;19:1922.
[30] Li GL, Yang XL, Bai F. Polymer 2007;48:3074.
[31] Bai F, Huang B, Yang XL, Huang WQ. Eur Polym J 2007;43:3923.
[32] Li GL, Song YY, Yang XL, Huang WQ. J Appl Polym Sci 2007;104:1350.
[33] Bai F, Yang XL, Huang WQ. Macromolecules 2004;37:9746–52.
[34] Fu GD, Shang Z, Hong L, Kang ET, Neoh G. Macromolecules 2005;38:7867.
[35] Yang M, Ma J, Yang ZZ, Lu YF. Angew Chem Int Ed 2005;44:6727.
[36] Wan X, Tu Y, Zhang D, Zhou Q, Wu C. J Am Chem Soc 2000;122:10201.
[37] Wu C, Zuo J, Chu B. Macromolecules 1989;22:633.
[38] Feldstein MM, Kiseleva TI, Bondarenko GN, Kostina JV. J Appl Polym Sci 2009;112:1142.
[39] Velasco-Santos C, Martnez-Hernndez AL, Castao VM. J Phys Chem B 2005;108:18866.